2021 43rd Annual International Conference of the
IEEE Engineering in Medicine & Biology Society (EMBC)
Oct 31 - Nov 4, 2021. Virtual Conference

Optimization framework for the model-based estimation of *in vivo* α-motoneuron properties in the intact human

R. Ornelas Kobayashi, A. Gogeascoechea, J. Buitenweg, U. Yavuz, M. Sartori

***Abstract*— The *in vivo* estimation of α-motoneuron (MN) properties in humans is crucial to characterize the effect that neurorehabilitation technologies may elicit over the composite neuro-musculoskeletal system. Here, we combine biophysical neuronal modelling, high-density electromyography and convolutive blind-source separation along with numerical optimization to estimate geometrical and electrophysiological properties of *in vivo* decoded human MNs. The proposed methodology implements multi-objective optimization to automatically tune ionic channels conductance and soma size of MN models for minimizing the error between several features of simulated and *in vivo* decoded MN spike trains. This approach will open new avenues for the closed-loop control of motor restorative technologies such as wearable robots and neuromodulation devices.**

***Clinical Relevance*— This work proposes a non-invasive framework for the *in vivo* estimation of person-specific α-motoneuron properties. This will enable predicting neuronal adaptations in response to neurorehabilitation therapies in the intact human.**

I. Introduction

Neurorehabilitation technologies (*e.g.*, robotic exoskeletons, transcutaneous electrical stimulation) aim at restoring the physiological function of the neuro-musculoskeletal system following neuromuscular lesions. However, the application of these technologies remains highly empirical [1], [2] due to the inability to measure the activity of the neural circuitries involved in the generation of movement. Moreover, the large anatomical variability among individuals makes it difficult to predict the neuromechanical response to a given therapy. As such, it is currently not possible to tailor rehabilitation therapies for person-specific needs.

In this context, studying the firing behavior of alpha-motoneurons (MNs), which represent the final common pathway of motor command computed by the central nervous system, is crucial to characterize the motor effect that neurorehabilitation technologies may elicit.

The output spike train produced by any neuron in response to an injected soma current is determined by the morphological and electrophysiological properties of such neuron [3]. This relationship can be quantified using biophysical models based on Hodgkin-Huxley formalism [4], where model parameters are tuned to produce the same firing pattern as experimentally measured neurons activity [5].

The complexity of *in silico* neuron models can range from single compartmental representations [6] to highly realistic three-dimensional models with multiple compartments [7]. Two-compartment models [8], where one compartment represents the soma and another the dendrites, are particularly relevant for the study of behavioral dynamics on relatively large MNs populations. Computational studies used this modelling approach to demonstrate the role of passive and active dendrites properties [9], calcium-mediated persistent inward currents [10], the influence that the common synaptic input to the MN pool has on force modulation [11] and torque [12], as well as the neural response to transcutaneous spinal cord stimulation [13]. However, these studies used model parameters based on generic data derived mainly from animal experimentation [8]. This limits their translation into clinic, mainly because none of them accounted for anatomical differences among individuals, nor were bounded to track experimental MNs discharge patterns. Although several optimization approaches have been proposed to match neuron models to experimental MN data, [14]–[16], they are restrained to *in vitro* conditions were both MNs output and input current are either known or measurable.

Advanced signal measurement and processing techniques [17] make it possible to decode the firing behavior of *in vivo* MNs from non-invasive high-density electromyogram recordings (HD-EMG). However, because the input received by the MN pool cannot be measured experimentally, the *in vivo* estimation of MN parameters remains an open challenge.

With the goal of overcoming current model limitations and enabling the subject-specific estimation of *in vivo* human MNs properties, we hereby present the first optimization framework to automatically tune electrophysiological and anatomical parameters of MNs models to match the firing behavior of *in vivo* human MNs decoded from HD-EMG.

Preliminary results demonstrate the potential of the proposed framework to estimate *in vivo* MNs properties, which opens a window for neurorehabilitation technologies to quantify potential neural adaptations elicited by a given therapy.

* Research supported by the European Research Council Starting Grant INTERACT (grant no. 803035).

R. Ornelas Kobayashi. A. Gogeascoechea and M. Sartori are with the Department of Biomechanical Engineering, University of Twente, Netherlands (email: r.e.ornelaskobayashi@utwente.nl).

U. S. Yavuz and J. Buitenweg are with the Biomedical Signals and Systems Group, University of Twente.

II. METHODS

A. Experimental recordings

Experiments were performed on a subject seating on a customizable chair, with the right leg fixed at a 90 degrees hip angle and the foot tightly strapped to a dynamometer for measuring ankle plantar-dorsi flexion torque during sustained isometric contractions at 20% of the maximum voluntary contraction (MVC). Dynamometer data was recorded in synchrony with HD-EMG (TMSi Refa multi-channel amplifier) from tibialis anterior (TA) muscle at a sampling frequency of 2048Hz. HD-EMG recordings from 64 channels were decomposed into individual MNs spike trains using Convolution Kernel Compensation (CKC) blind source separation algorithm [18]. Resulting spike trains consisted of one-dimensional binary arrays where 1 represented a spike time and 0 no activity.

B. Common input current estimation

Measuring the current input at the MN soma during *in vivo* conditions is one of the biggest challenges for fitting neuron models. Computational evidence [19] has suggested that the neural drive to muscle, which represents the net firing activity of the MN pool innervating a muscle, is a linear transformation of the low frequency components of the common synaptic input received by the MN pool. Inversely, this means that a low-pass filtered common synaptic input could be approximated from the net firing activity of the MN pool. As described by Sartori et al [17], we estimated the discharge rate of the *in vivo* decoded MNs using equation (1), where t_n represents the discharge time on the n^{th} spike in the cumulative train. The discharge rate was smoothed by a moving average window of 500 samples to obtain an estimate of the net firing activity of the *in vivo* MN pool.

$$DR_n = \frac{1}{t_n - t_{n-1}} \quad (1)$$

Z-score normalization was then applied to obtain a zero mean net activity profile. Subsequently, MN pool mean firing frequency and standard deviation (SD) were calculated from the concatenated spike train of all decoded MNs outputs. Adding the product between the net activity profile and SD to the MN pool mean firing frequency, we generated a signal $f(t)$ that captures the net firing activity of the MN pool.

Taking advantage of the linear current-frequency relationship described by literature in MNs firing below 40Hz [3], we estimated the common *in vivo* soma current received by the MNs pool (2) using ΔIF as an empirical slope value for the linear region of the current-frequency curve [20].

$$I(t) = f(t) * \Delta IF \begin{cases} \Delta IF = 0.25, & f(t) \leq 25 \\ \Delta IF = 0.75, & f(t) > 25 \end{cases} \quad (2)$$

B. Motoneuron model

The implemented model was based on the two-compartment description of Cisi and Kohn [8]. Since this approach consisted of injecting the common input current into the soma, dendrite compartment was removed, whereas geometric and electro-physiological parameters of the soma remained the same. Four parameters were the exception: maximum conductance of fast and slow potassium channels (gK_f and gK_s, respectively), peak value at pulse activation (β_Q) and soma diameter. The value of these parameters was determined using multi-objective optimization (section II.D). Parameters choice and upper/lower boundaries were based on updated tables from the original model [21] to maximize MN-type classification (*e.g.* potassium-related properties vary across MN types, unlike sodium [21]) and ensure physiologically realistic values with a minimum amount of parameters (*e.g.* rate constant β dominates α during potassium pulse generation [22]).

D. Optimization algorithm

Since single optimization is affected by unequal contributions of different features to the objective function [14], we implemented multiple-objective optimization (MOO) using global optimum determination by linking and interchanging kindred evaluators (GODLIKE) [23]. GODLIKE is a highly robust algorithm that simultaneously executes relatively simple implementations of genetic algorithm, differential evolution, particle swarm and adaptive simulated annealing. When any aforementioned method converges, GODLIKE randomly interchanges the members of each population and proceeds with optimization.

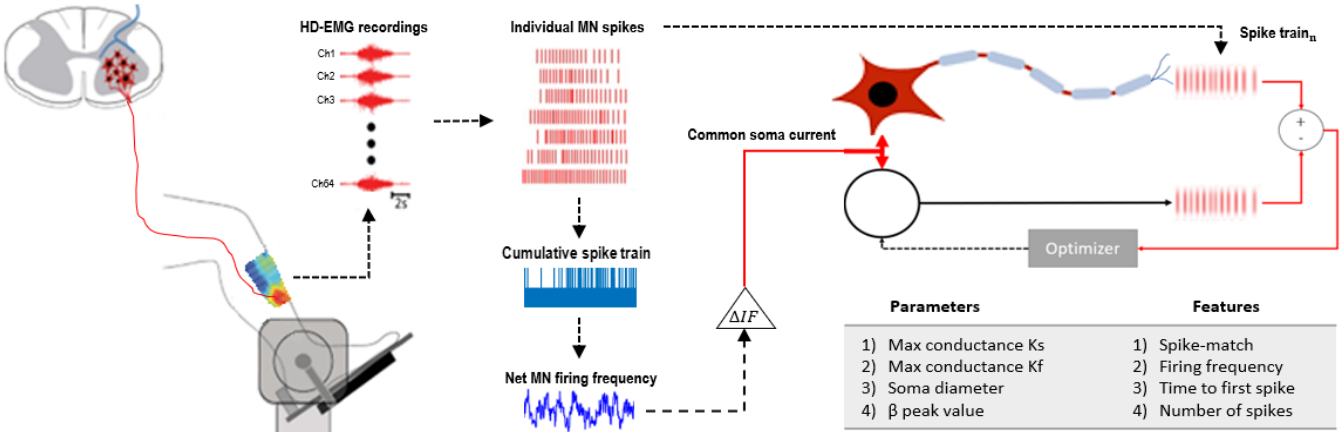

Figure 1. *In vivo* MN spike trains are decomposed from HD-EMG recordings and the net MN pool firing frequency is calculated. Common soma current is derived from the product of net firing frequency and current-frequency slope (ΔIF). Optimization is then executed for each decoded MN spike train taking the same common current as input. Optimization tunes model parameters to reproduce *in vivo* MN spikes minimizing the error of four features: spike time match, mean firing frequency and time to first spike and number of spikes.

Four objective functions where defined: spike-match [24] (3), mean firing frequency error (4), first spike error (5) and spikes number correction (6):

$$1 - \frac{2}{1-2\delta f_e}\left(\frac{N_c - 2\delta f_e N_e}{N_e + N_m}\right) \quad (3)$$

$$2\left|\frac{f_e - f_m}{f_e}\right| \quad (4)$$

$$2\left|\frac{train_e(i) - train_m(i)}{train_e(i)}\right|_{i=1} \quad (5)$$

$$\left|\frac{N_e - N_m}{N_e}\right| \quad (6)$$

Where f_e and f_m are mean firing rate [Hz], N_e and N_m number of spikes, and $train_e$ and $train_m$ the spike times [ms] of experimental and modelled MNs, respectively. N_c is number of coincident spikes withing a time window of δ = 2ms [24].

GODLIKE algorithm was executed until finding the dominant set of parameters that equally minimized all four objective functions. Subsequently, similarity between *in vivo* and *in silico* MN spike trains was quantified using the coincidence factor Γ [24], where Γ = 1 means perfect match and Γ < 0.1 is considered random chance. Lastly, a sensitivity analysis was performed measuring the change in the objective functions relative to each parameter. This was done taking the optimized sets of parameters for each MN but varying one parameter at the time across its entire range.

III. RESULTS

The spike trains produced by the *in silico* MNs models after MOO were very similar to their corresponding *in vivo* MNs twins (Fig 2). Parameter optimization resulted in Γ ≈ 0.2, while generic parameters yielded Γ < 0.01 (Fig 3).

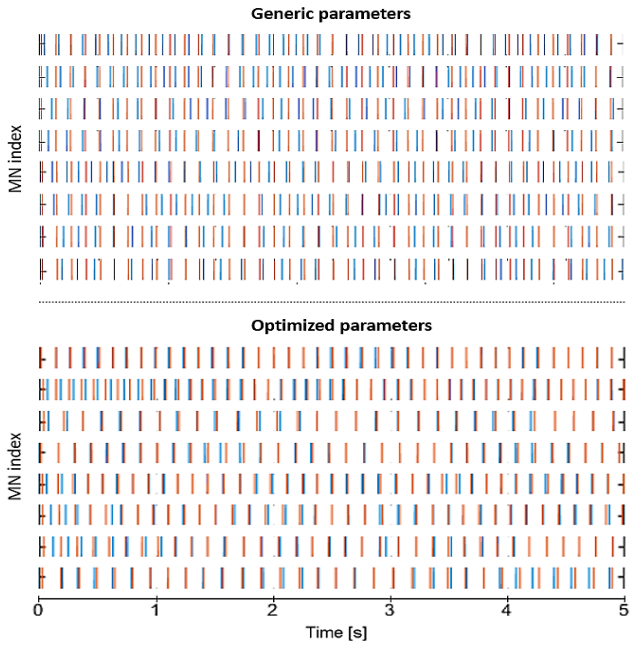

Figure 2. **Blue:** *in vivo* MNs spike trains decoded from HD-EMG **Orange:** spike trains produced by *in silico* MNs after MMO.

Sensitivity analysis (Fig 4) showed that, with exception of gK_f, all selected parameters have an optimal value where objective functions are minimized. Notably, gK_s and β_Q have a high impact over firing frequency and spikes number error, while diameter alone determines time to first spike error. Range and distribution of all MOO identified parameters are summarized in Fig 5.

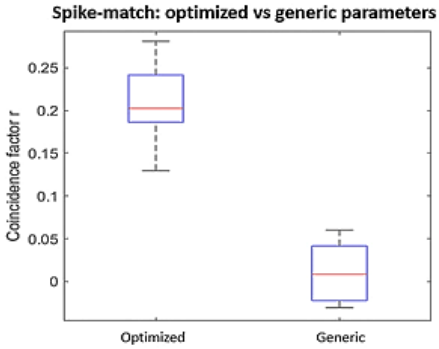

Figure 3. coincidence factor for generic and optimized MN parameters

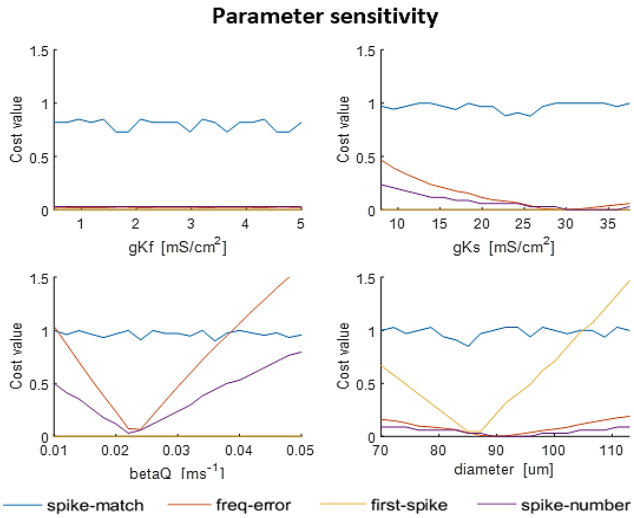

Figure 4. Parameter sensitivity analysis show that, with the exception of gK_f, all selected parameters have an optimal value where the objective functions are minimized for each MN. Parameters shown are from MN7.

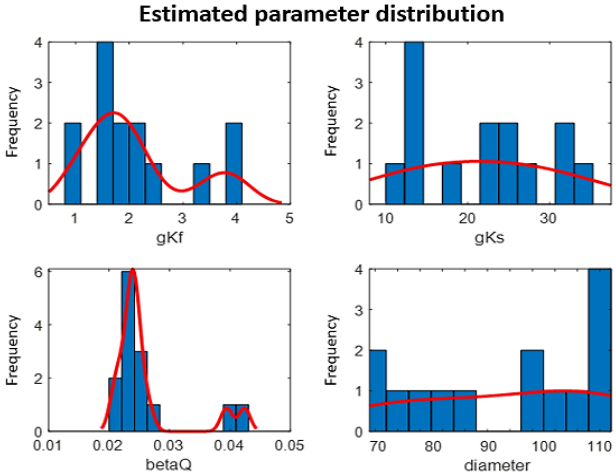

Figure 5. Histogram of MN parameters identified by MOO framework.

IV. DISCUSSION

The high influence of the soma diameter over the first spike time feature goes in line with Henneman's size principle [25], which dictates that MNs are recruited by their order of size. MOO identified parameters (Fig 4) seem to suggest a relatively uniform distribution of MN sizes. However, this is a limitation in our data: *in vivo* MN spike trains were taken when the subject was already at 20% MVC. Thus, the first spike used as reference for optimization was not representative of MNs recruitment. Future work should include data from the rising time of the force, where the real first recruitment spike could be estimated. Moreover, because only data from 20% MVC was considered, it is likely that only small size (*i.e.,* slow) MNs were included in this study. Experimental data including ramps from zero to higher %MVC steady values could allow the identification of larger MNs (*i.e.,* fatigue resistant and fast fatigable), potentially enabling *in vivo* MN classification.

The electrophysiological properties of slow potassium channels (gK_s and β_Q) are highly sensitive parameters determining firing frequency and number of spikes features. Since both features are closely related, future work should only consider firing frequency, as it accounts for larger changes in the cost function than the spike number feature.

Besides some fluctuations in the spike-match function, fast potassium channels (gK_s) did not show any sensitivity towards any feature. This suggests that electrophysiological properties of slow potassium channels, together with soma size, may be enough parameters for reliable MN optimization. However, future work should explore different objective functions (*e.g.* cross-correlation, van Rossum metric) to maximize spike match and validate parameter selection. It is worth mentioning that the empirical slope values (section II.B) for estimating the common input current may require further validation. Future work could focus on optimizing these parameters from the frequency-current curve.

V. CONCLUSION

Despite data limitations, preliminary results demonstrate the potential of the proposed optimization framework for estimating *in vivo* MNs properties derived from HD-EMG.

REFERENCES

[1] A. Megía García, D. Serrano-Muñoz, J. Taylor, J. Avendaño-Coy, and J. Gómez-Soriano, "Transcutaneous Spinal Cord Stimulation and Motor Rehabilitation in Spinal Cord Injury: A Systematic Review," *Neurorehabil. Neural Repair*, vol. 34, no. 1, pp. 3–12, 2020, doi: 10.1177/1545968319893298.

[2] N. Takeuchi and S. Izumi, "Rehabilitation with Poststroke Motor Recovery: A Review with a Focus on Neural Plasticity," *Stroke Res. Treat.*, vol. 2013, 2013.

[3] R. Granit, D. Kernell, and G. K. Shortess, "Quantitative aspects of repetitive firing of mammalian motoneurones, caused by injected currents," *J. Physiol.*, pp. 911–931, 1963.

[4] A. L. Hodgkin and A. F. Huxley, "A quantitative description of membrane current and its application to conduction and excitation in nerve," *J. Physiol.*, vol. 117, pp. 500–544, 1952.

[5] C. Rossant, D. F. M. Goodman, J. Platkiewicz, and R. Brette, "Automatic fi tting of spiking neuron models to electrophysiological recordings," vol. 4, no. March, pp. 1–10, 2010, doi: 10.3389/neuro.11.002.2010.

[6] D. Haufler, F. Morin, J. C. Lacaille, and F. K. Skinner, "Parameter estimation in single-compartment neuron models using a synchronization-based method," vol. 70, pp. 1605–1610, 2007, doi: 10.1016/j.neucom.2006.10.041.

[7] P. Balbi, S. Martinoia, and P. Massobrio, "Axon-somatic back-propagation in detailed models of spinal alpha motoneurons," *Front. Comput. Neurosci.*, vol. 9, no. JAN, pp. 1–11, 2015, doi: 10.3389/fncom.2015.00015.

[8] R. R. L. Cisi and A. F. Kohn, "Simulation system of spinal cord motor nuclei and associated nerves and muscles , in a Web-based architecture," pp. 520–542, 2008, doi: 10.1007/s10827-008-0092-8.

[9] L. A. Elias and V. M. Chaud, "Models of passive and active dendrite motoneuron pools and their differences in muscle force control," pp. 515–531, 2012, doi: 10.1007/s10827-012-0398-4.

[10] C. J. Heckman, M. Johnson, C. Mottram, and J. Schuster, "Persistent Inward Currents in Spinal Motoneurons and Their Influence on Human Motoneuron Firing Patterns," vol. 14, no. 3, 2008, doi: 10.1177/1073858408314986.

[11] J. L. Dideriksen, S. Muceli, S. Dosen, C. M. Laine, and D. Farina, "Physiological recruitment of motor units by high-frequency electrical stimulation of afferent pathways," *J. Appl. Physiol.*, vol. 118, no. 3, pp. 365–376, 2015, doi: 10.1152/japplphysiol.00327.2014.

[12] R. N. Watanabe, F. H. Magalhães, L. A. Elias, V. M. Chaud, E. M. Mello, and A. F. Kohn, "Influences of premotoneuronal command statistics on the scaling of motor output variability during isometric plantar flexion," *J. Neurophysiol.*, vol. 110, no. 11, pp. 2592–2606, 2013, doi: 10.1152/jn.00073.2013.

[13] A. Kuck, D. F. Stegeman, and E. H. F. Van Asseldonk, "Modeling trans-spinal direct current stimulation for the modulation of the lumbar spinal motor pathways," *J. Neural Eng.*, vol. 14, no. 5, 2017, doi: 10.1088/1741-2552/aa7960.

[14] S. Druckmann, Y. Banitt, A. Gidon, F. Sch, and H. Markram, "A novel multiple objective optimization framework for constraining conductance-based neuron models," vol. 1, no. 1, 2007.

[15] S. Masoli, M. F. Rizza, M. Sgritta, W. Van Geit, F. Schürmann, and E. D. Angelo, "Single Neuron Optimization as a Basis for Accurate Biophysical Modeling : The Case of Cerebellar Granule Cells," vol. 11, no. March, pp. 1–14, 2017, doi: 10.3389/fncel.2017.00071.

[16] S. Hill, H. Markram, I. Segev, S. Druckmann, T. K. Berger, and F. Schu, "Effective Stimuli for Constructing Reliable Neuron Models," vol. 7, no. 8, 2011, doi: 10.1371/journal.pcbi.1002133.

[17] M. Sartori, U. Ş. Yavuz, and D. Farina, "In Vivo Neuromechanics : Decoding Causal Motor Neuron Behavior with Resulting Musculoskeletal Function," no. September, pp. 1–14, 2017, doi: 10.1038/s41598-017-13766-6.

[18] A. Holobar, "Accurate identification of motor unit discharge patterns from high-density surface EMG and validation with a novel signal-based performance metric," 2014, doi: 10.1088/1741-2560/11/1/016008.

[19] D. Farina and F. Negro, "Common Synaptic Input to Motor Neurons , Motor Unit Synchronization , and Force Control," no. 5, pp. 23–33, 2015.

[20] K. D. B. Powers and M. D. Binder, "Experimental Evaluation of Input-Output Motoneuron Discharge Models of," vol. 75, no. 1, pp. 367–379, 2018.

[21] F. Kohn and L. Abdala, "Individual and collective properties of computationally efficient motoneuron models of types S and F with active dendrites," vol. 99, pp. 521–533, 2013, doi: 10.1016/j.neucom.2012.06.038.

[22] A. Destexhe, "Conductance-Based Integrate-and-Fire Models," no. May 1997, 2015, doi: 10.1162/neco.1997.9.3.503.

[23] R. Oldenhuis, "GODLIKE—a robust single-& multi-objective optimizer," 2017. [Online]. Available: https://nl.mathworks.com/matlabcentral/fileexchange/24838-godlike-a-robust-single-multi-objective-optimizer. [Accessed: 06-Apr-2021].

[24] E. P. Lynch and C. J. Houghton, "Parameter estimation of neuron models using in-vitro and in-vivo electrophysiological data," vol. 9, no. April, pp. 1–15, 2015, doi: 10.3389/fninf.2015.00010.

[25] E. Hennema, G. Somjen, and D. O. Carpenter, "Functional significance of cell size in spinal motoneurons," *J Neuorphysiol*, 1965, doi: doi: 10.1152/jn.1965.28.3.560.